

## Recent development in grain refinement by hydrostatic extrusion

Malgorzata Lewandowska · Krzysztof J. Kurzydłowski

Received: 5 March 2008 / Accepted: 16 June 2008 / Published online: 26 July 2008  
© Springer Science+Business Media, LLC 2008

**Abstract** Hydrostatic extrusion is an efficient method of grain refinement to the nanometer scale in metallic materials. The paper shows that it can be used directly to obtain a mean grain size smaller than 100 nm with a significant fraction of high angle grain boundaries in aluminum alloys, titanium, and iron. It is also demonstrated that grain size reduction to this level in some other materials, e.g., nickel, requires a combination of hydrostatic extrusion (HE), as the final operation, after some other methods of severe plastic deformation (SPD). Grain refinement in metallic materials by HE has a significant effect on their properties with a significant increase in mechanical strength and improvement of wear and corrosion resistance while maintaining an acceptable level of plasticity.

### Introduction

Recently the growing interest in nano-materials has stimulated research and development on the methods to achieve grain refinement in metals. Various techniques, which can be used to refine the size of grains in polycrystalline material to below 100 nm, have been proposed in this context. A large group of these methods is based on the assumption that severe plastic deformation (SPD) enables micrograined aggregates to be transformed to the nano-size by the accumulation and rearrangement/annihilation of the crystal lattice defects, primarily dislocations. Experimental observations showed, that for such a transformation to take

place, a large degree of plastic deformation is required, which usually exceeds the maximum equivalent strain achievable in simple plastic forming methods [1, 2]. As a result, special deformation methods have been invented and employed, including equal channel angular pressing [3], high pressure torsion [4], cyclic extrusion compression [5], and multi-axes forging [6]. More recently, hydrostatic extrusion (HE) has been used for this purpose [7, 8].

In comparison to the standard SPD methods, the HE process, as a method of grain refinement, usually requires a significantly smaller total strain [9]. This is primarily due to the high strain rates, which frequently exceed  $10^2 \text{ s}^{-1}$  and reduce the extrusion time to seconds. As a result, the work associated with plastic deformation is more efficiently transformed into the energy of the accumulated defects. On the other hand, heat is released in the process but it has an impulse-like character and can be either reduced by cooling the product at the die exit or utilized as a post deformation treatment.

The aim of this paper is to review the recent results of the applications of HE for grain refinement. The reported results have been predominantly obtained by a group of scientists and engineers affiliated to the Center for Materials Extrusion established jointly by Warsaw University of Technology and the Institute of High Pressure Physics of the Polish Academy of Sciences. The focus of the following text is on the efficiency of grain refinement and the properties of the extruded materials. Technical details and more information on the activities of the Center can be found elsewhere [7–20].

### Efficiency of the grain refinement

A number of technically pure metals and alloys have been processed by HE at ambient temperature to evaluate the

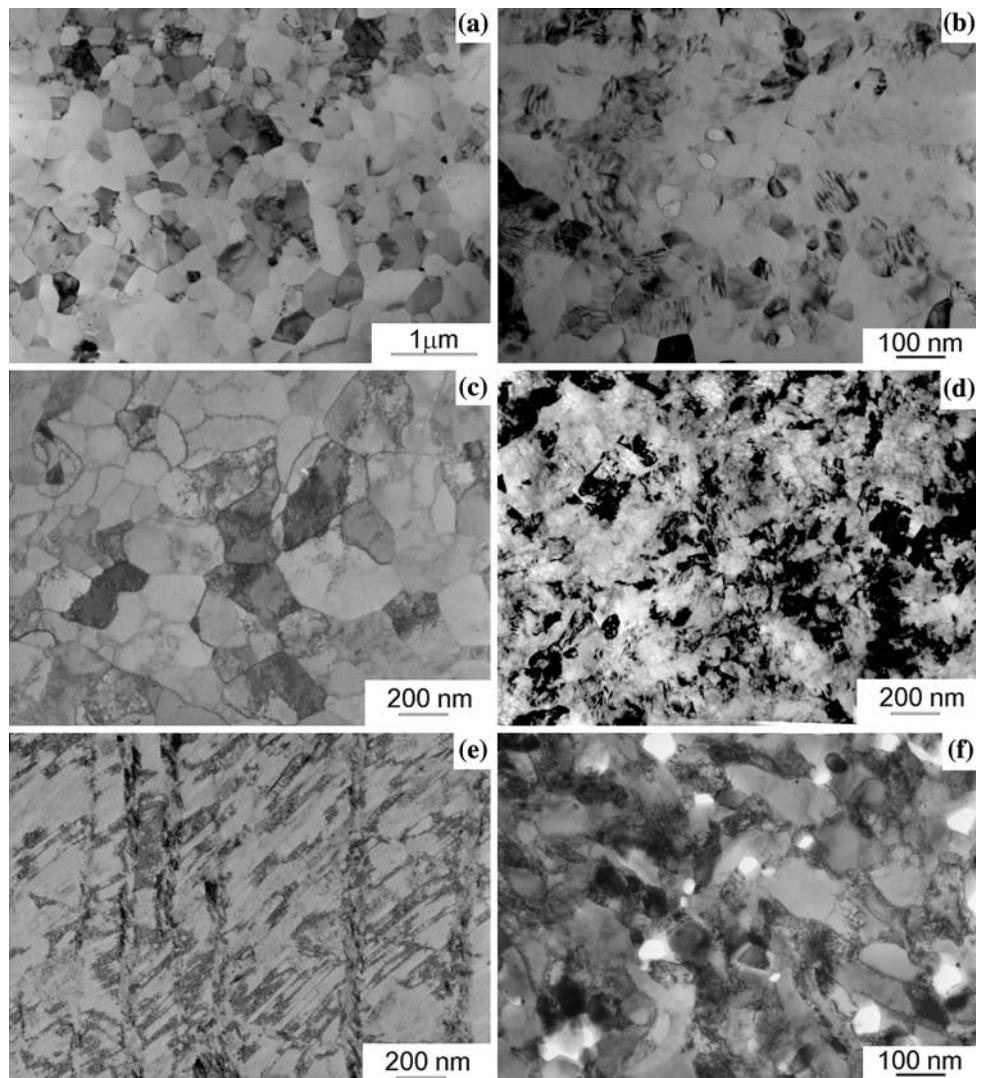
M. Lewandowska · K. J. Kurzydłowski (✉)  
Faculty of Materials Science and Engineering,  
Warsaw University of Technology, Woloska 141,  
02-504 Warszawa, Poland  
e-mail: kjk@inmat.pw.edu.pl

potential of this method for achieving grain size refinement. Comparative studies have been performed on aluminum alloys, which are used here for benchmarking the efficiency of grain refinement. Undertaking this benchmarking exercise, it must be stressed that HE brings about refined microstructures which significantly differ in their character, which are dependent on the materials being processed and the technological parameters of the process. The differences, in particular, concern the density of dislocations inside the refined grains, the character of the grain boundaries and the size of grains. Some of the most characteristic microstructures obtained by HE are shown in Fig. 1. In the case of pure aluminum (Fig. 1a), equiaxed grains, almost free of dislocations, can be observed whereas in pure copper (Fig. 1b) a dislocation cell structure is present after the same true strain. Grain refinement is much more efficient in the case of aluminum alloys (Fig. 1c, d). However, their grain interiors contain a significant density of dislocations. Hydrostatically extruded

stainless steel (Fig. 1e) exhibits a different microstructure composed of nano-twins.

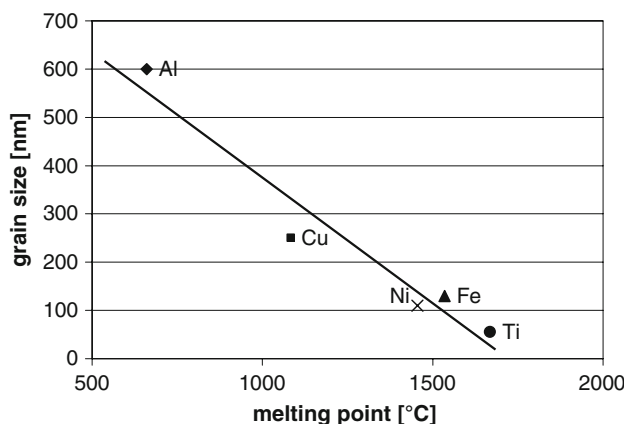
To characterize the efficiency of grain refinement, the microstructures of various HE processed materials have been analyzed in terms of the equivalent diameter,  $d$ , for the population of grains/subgrains revealed by TEM. The mean values of equivalent diameter,  $E(d)$ , for various materials are listed in Table 1. For pure metals, the lowest degree of grain size refinement was achieved in pure aluminum whereas the highest was in pure titanium. This finding indicates that the efficiency of HE carried out at room temperature increases with the increasing melting point of the materials being processed as established in the plot of grain size versus melting temperature (Fig. 2). This is fully understandable in view of the contribution of the thermally activated processes of recovery and recrystallization, which take place either during extrusion or soon after its completion. As a result, the efficient processing of low melting point materials may require the billets to be

**Fig. 1** Microstructures of HE processed materials: (a) aluminum, (b) 2017 aluminum alloy, (c) copper, (d) titanium, (e) austenitic stainless steel, and (f) Eurofer 97 steel. All materials were HE processed with a total true strain of  $\sim 4$



**Table 1** The equivalent total strain and average grain size for various materials processed by HE

Material	Equivalent strain	Initial grain size (μm)	Final grain size (nm)	Ref.
Aluminum 1050	3.8	1	600	[10]
Aluminum 2017	3.8	20	95	[11]
Aluminum 7475	3.8	74	66	Lewandowska, Unpublished work
Aluminum 5186	3.8	320	105	[12]
Aluminum 6082	3.8	2.5	195	[13]
Copper	3.8	40	250	Lewandowska, Unpublished work
Nickel	13.5	40	100	[14]
Titanium	3.8	12	55	[15]
Austenitic stainless steel	1.8	Microtwins	Nano-twins	[16]
Eurofer 97 steel	3.9	0.5	60	[17]

**Fig. 2** Mean grain diameters of HE processed pure metals plotted as a function of their melting temperature

cooled prior to processing and/or the extruded material cooled at the die exit. The efficiency of HE is much higher in the case of alloys (in particular aluminum alloys) where the presence of alloying elements strongly decrease the rate of recovery. As a result, the grain size decreases continuously and is finer for alloys with a higher content of alloying elements (see Table 1).

Systematic studies of the final grain size as a function of the total strain accumulated in HE indicate that the most rapid refinement takes place at a relatively low strain [18]. At larger strains grain size changes occur slowly approaching some limiting value for any given material. However, a further substantial decrease in the grain size can be achieved by combining HE with other SPD methods as has been demonstrated for Cu and Ni [19].

### High angle grain boundaries

As the properties of polycrystalline materials depend not only on the size of grains, but also on the character of the grain boundaries, the process of hydrostatic extrusion

**Table 2** Grain size and the fraction of high angle grain boundaries for pure aluminum processed by various methods of SPD

	ECAP	CEC	ARB	CR	HE
True strain	8	60	6	5	4
Grain size (nm)	300–1000	1200	1000	300	600
HAGB (%)	65	60	70	60	60
Ref.	[3]	[5]	[20]	[21]	[10]

should also be evaluated in terms of the potential for the formation of high angle grain boundaries. This is relevant particularly for nano-materials obtained by plastic deformation, which tend to exhibit a high fraction of low angle grain boundaries.

Systematic studies of the formation of high angle grain boundaries in HE have been carried out on 1050 aluminum alloy. The microstructure of the extruded material is shown in Fig. 1a. Grain boundary mis-orientation angles were measured from the Kikuchi line patterns obtained by TEM. (For more details, see [10]). The measured fractions of the high angle grain boundaries are listed in Table 2 and compared to the results obtained for aluminum processed by other methods of severe plastic deformation. The data clearly indicate that, in the case of hydrostatic extrusion, similar refinement of the microstructure is achieved after a significantly lower accumulated strain.

### Grain size diversity

In general nano-metals obtained by plastic deformation exhibit a considerable degree of grain size diversity. This is due to the stochastic nature of the formation and growth of nano-grains during the process of plastic deformation, which is unlike low temperature consolidation of powders as they can be sieved to obtain grains/particles of uniform size.

The grain size diversity can be quantified in terms of the equivalent diameter  $CV(d)$  coefficient of variation. This

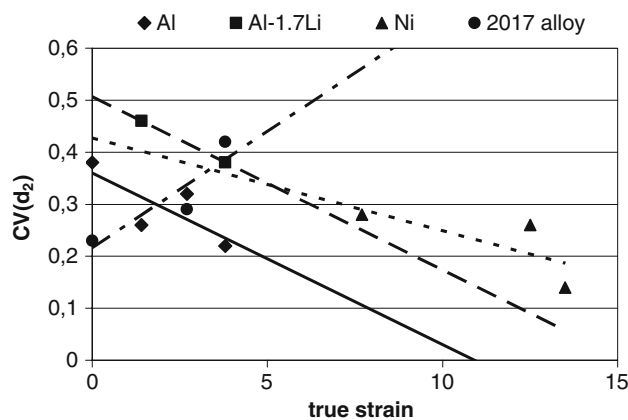


**Fig. 3** Values of variation coefficient  $CV(d)$  as a function of true strain in various materials processed by hydrostatic extrusion. The lines are drawn through the points obtained in one series of experiments. They indicate that with increasing true strain,  $CV$  generally decreases (the opposite has been observed for 2017 aluminum alloy)

parameter, defined as the ratio of the standard deviation to the mean value, is circa 0.2 for fairly uniform grain structures, (for more information see [22]), but for HE processed metals it ranges from 0.2 to 0.5 depending on the material and processing parameters—see Fig. 3. It is not easy to compare grain size diversity of HE processed material with that produced by other SPD techniques as data are relatively scarce.

## Second phase particles

The engineering materials, including those which are theoretically single-phased, usually contain particles of a second phase. Such phases include primary intermetallic inclusions resulting from the presence of impurities and precipitates which form during the heat treatment. The role of these two types of particles on grain refinement was studied in experiments carried out on 7475 aluminum alloy.

Samples of the alloy samples having different microstructures as a result of heat treatment were HE processed. Prior to HE the samples possessed the following combinations of inclusions and precipitates:

- (1) low density inclusions (solution heat treated samples),
- (2) low density inclusions and low density large precipitates (annealed samples), and
- (3) low density inclusions and high density small precipitates (solution heat treated and aged).

It was found that the smallest grain size, with a mean value of  $\sim 60$  nm, was obtained in the annealed sample (2)—Fig. 4b. The 7475 aluminum alloy, when processed immediately after water quenching, exhibits a well-developed microstructure with a grain size of 90 nm (Fig. 4a). The

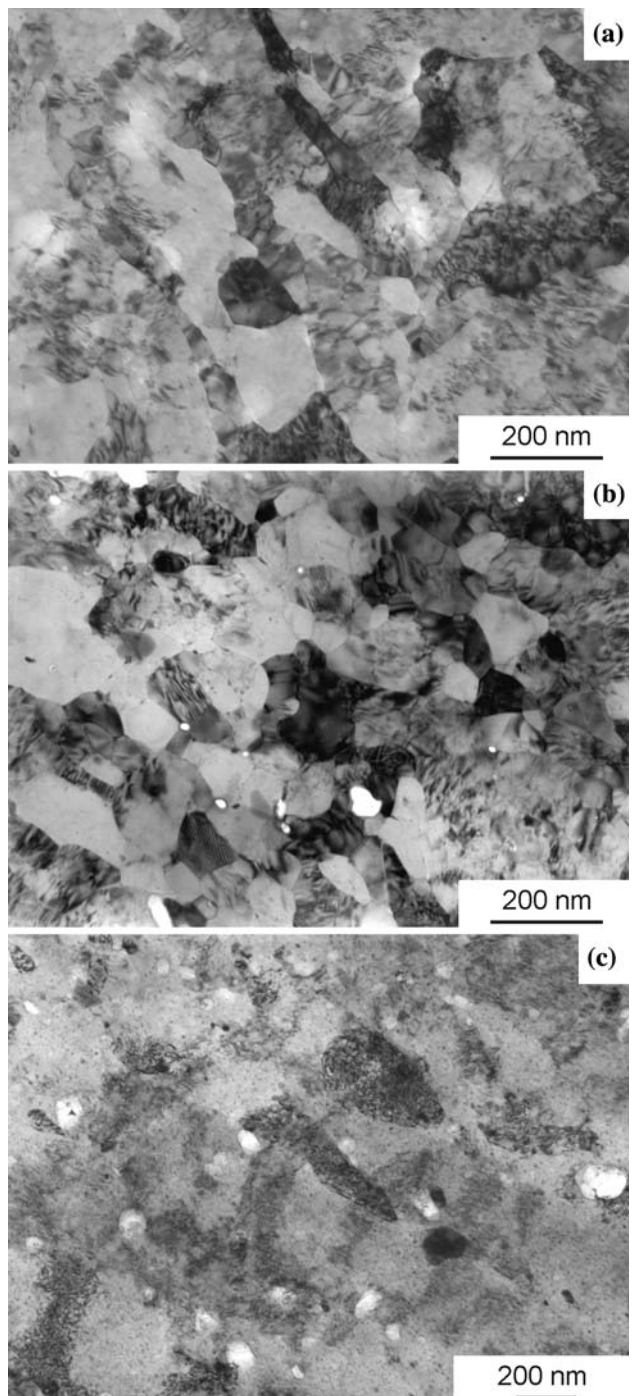


**Fig. 4** Microstructures of HE processed 7475 alloy after pre-treatment: (a) solution heat treated and water quenched, (b) annealed, and (c) solution heat treated and aged. The influence of second phase particles on grain refinement is shown (for details see text)

same alloy processed after aging has a microstructure containing a high density of dislocations with much less developed larger grains (Fig. 4c).

This results indicate that relatively large precipitates resisting plastic deformation accelerate grain refinement

**Table 3** Stereological parameters of intermetallic inclusions before and after hydrostatic extrusion: mean particle diameter,  $E(d_p)$ , shape factors  $\alpha$  and  $\beta$ , variation coefficient of interparticle distance  $CV(l)$ 

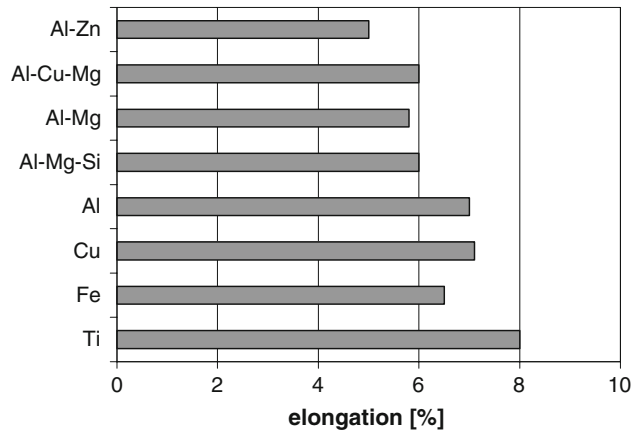
	$E(d_p)$ ( $\mu\text{m}$ )	$\alpha = d_{\max}/d_{\text{eq}}$	$\beta = p/\pi d_{\text{eq}}$	$CV(l)$
Before HE	1.4	1.41	1.23	0.57
After HE	1.22	1.34	1.18	0.34

whereas small precipitates inhibit the formation of the nanostructure. This results are in good agreement with those reported in [23, 24] and previously obtained with 2017 aluminum alloy [8].

In addition to the second phase particles influencing the process of grain refinement, they also undergo changes during processing [11]. Relatively large and thermodynamically stable inclusions are slightly reduced in size, but are distributed significantly more uniformly. Table 3 shows the mean values of particle diameter and their shape factors as well as the variation coefficient of the distance between particles, this parameter quantifies the homogeneity of the spatial distribution of the particles. Small and meta-stable precipitates may transform/dissolve due to shearing by moving dislocations and/or thermal effects (adiabatic heating) caused by HE processing.

### Mechanical properties of HE processed metals

Grain refinement taking place in metals due to HE processing has a significant impact on the mechanical properties. The yield strength for a number of engineering materials in their conventional and nano-structured forms are given in Table 4. It can be noted that in the case of technically pure nano-structured titanium, a yield strength of more than 1000 MPa was achieved, which is typically the value exhibited by titanium alloys. For single phase nano-structured 5XXX aluminum alloy, a yield strength of 485 MPa was obtained which is similar to conventional age-hardened aluminum alloys. Precipitation hardened nano-structured 2XXX aluminum alloy after HE has a strength similar to that possessed by conventional 7XXX alloys, which are considered to be the strongest of the aluminum alloys. These results clearly confirm the potential of HE as a method for improving the mechanical strength of metals without changing their chemistry.

**Fig. 5** Ductility of materials processed by hydrostatic extrusion

Although nano-structured metals exhibit excellent strength, their industrial use is currently limited by their low level of ductility. Conventional work-hardening, which is in a sense a processing reference for SPD methods, can result in the ductility being reduced to given an elongation of only 1% in a tensile test. The formation of nano-grain structures in SPD metals not only enhances strength, but also the ductility is considerably enhanced, as seen from the data given in Fig. 5 for HE processed metals. However, the ductility still remains below the level typical of samples with a conventional grain size (although it is significantly higher than in the case of nano-metals obtained by electro-deposition [25]). It can be seen that the ductility of hydrostatically extruded materials is fairly good in the absence of any post-processing. In the case of high melting point metals, it can be further increased by low temperature annealing.

The nano-grain size samples strained to fracture show a high tendency for strain localization. This tendency can be explained in terms of the mechanical instability occurring during tensile testing. In such a case, the low elongation to fracture does not imply an inherent brittleness of SPD metals. However, the use of SPD nano-metals for the fabrication of structural parts may require different design rules.

### Thermal stability

One of the most important requirements of engineering materials is thermal stability of their microstructure/

**Table 4** The yield strength (MPa) for engineering materials with micrometric and nanometer grain size

Structure	Ti	Ni	5483 Al alloy	2017 Al alloy	7475 Al alloy	Austenitic steel	Eurofer 97 steel
Microscale	345	270	147	320	230	965	555
Nanoscale	1060	926	485	570	650	1658	1641
Ref.	[15]	[14]	[12]	[8]	Lewandowska, Unpublished work	[16]	[17]

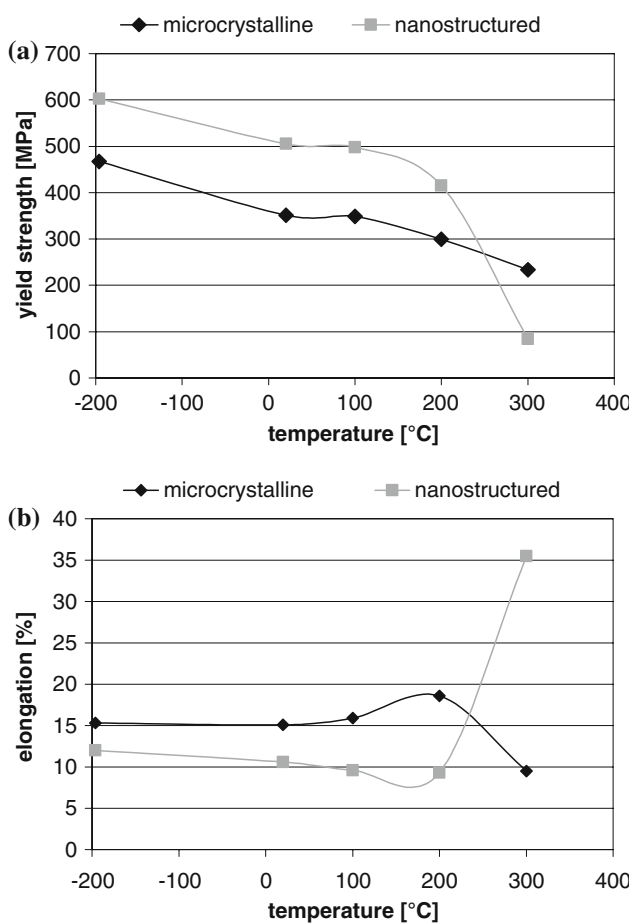


**Fig. 6** Yield strength (a) and elongation (b) as a function of temperature for microcrystalline and nano-structured Al–Cu alloy

properties. However, nano-grained metals are inherently thermodynamically unstable due to the high accumulation of defects (particularly in the form of grain boundaries). The mechanical properties of nano-Al–Cu alloy obtained by HE were measured over a wide range of test temperatures and compared to the conventional micrograined alloys. The results are shown in Fig. 6. It may be noticed that the nano-material has a higher yield strength from the cryogenic temperature to 150 °C with the yield stress dependence on test temperature following the same pattern as for the micrograined alloy. At the temperature of 200 °C, a significant decrease in the strength of the nano-alloy is observed. Above this temperature, the flow stress of the nano-grained material decreases rapidly, as would be expected from the basic theories of metallurgy.

The results obtained on the Al–Cu alloy clearly show that nano-grained metals obtained by HE and most likely by other SPD metals, retain their superior properties over a well-specified range of temperature. Such data will need to be established for each material prior its wider industrial application.

**Table 5** Tribological properties of an austenitic stainless steel evaluated by the pin-on-disc method (counterpart specimen NC6 steel, load 13.3 MPa, speed 0.04 m/s, test duration 60 min)

Material	Test conditions	Surface roughness, $R_a$ (μm)		Friction coefficient $\mu$	Weight loss, g
		Before test	After test		
Before HE	Dry	0.12	1.8	0.39	0.0084
	Lubricated	0.12	2.5	0.28	0.005
After HE	Dry	0.03	1.5	0.39	0.0066
	Lubricated	0.09	0.4	0.009	0.0010

The results also show that the ductility of the nano-structured samples increases at cryogenic temperatures and approaches that of microcrystalline samples.

## Wear resistance

Modern engineering materials must possess desirable mechanical and functional properties. In particular, the specific physical and chemical properties which are required for advanced applications in such sectors as transport or bio-engineering.

Parameters defining the coefficient of friction and the wear resistance of nano-316LVM steel are given in Table 5. The surface roughness was described by  $R_a$ , the sum of the absolute values of all the areas above and below the mean line divided by the sampling length. As expected, the friction coefficient is lower for the lubricated condition. However, it is worth noting that the coefficients are smaller for the HE processed samples. These data indicate that the nano-grained form of this steel, widely used in biomedical applications, has enhanced wear resistance. HE has also a beneficial impact on the wear resistance of titanium. Particularly encouraging are the results of friction tests performed for HE processed pure titanium with a counter-specimen made of UHMWPE [26].

## Corrosion resistance

The results obtained on Ti and stainless steel [27, 28] show that the general corrosion resistance of HE processed samples exposed to a 0.9% NaCl solution remains good. At the same time, the tendency for pitting corrosion is significantly reduced. It has been also shown, that the naturally occurring oxide film on the HE processed 316L stainless steel contains a higher concentration of Cr, most likely due to its more rapid diffusion to the free surface.

Local corrosion measurements have shown that corrosion is initiated at the interface between the inclusions and

the steel. It was also revealed that some types of inclusions became inactive after HE processing due to the size refinement [29].

## Discussion and concluding remarks

The results clearly demonstrate that hydrostatic extrusion is an efficient method for grain refinement. Its advantages over standard SPD processes, such as ECAP and HPT, are the following:

- High refinement at relatively low final strain
- The possibility of processing hard-to-deform materials
- Relatively long processed elements
- The possibility of processing elements of different cross sections (rods, wires, and pipes)

The high efficiency of hydrostatic extrusion results from the specific deformation conditions which ensure a high rate of defect rearrangement and a rapid transformation of the microstructure from those characteristic for deformation into ultrafine/nano grained. In this context, high pressure and high strain rates play a key role. Both these factors accelerate the accumulation of defects. In addition, high strain rates make the process close to adiabatic which results in rapid heating. As a result, the heavily deformed microstructure transforms to nano-sized much more rapidly than in the SPD methods in which dissipation of energy takes long time and the temperature rise is negligible. It should also be noted that hydrostatic extrusion is very fast and as a consequence the heat release has an impulse-like character. Its duration can be further shortened by water cooling at the die exit.

Among the disadvantages, one should list:

- The need for high pressure facilities and equipment
- The reduction in the diameter/thickness of the processed billets

As a result, HE, although not being the SPD method, as a technique of choice should be generally taken into account in any development of industrial processes for nano-grain refinement. At this stage, it certainly can be used to test some of the limits of grain refinement via plastic deformation and the properties of metals refined to nano-size of grains.

One of the relatively new ideas, which emerged from the results obtained for aluminum alloys processed by HE, is the role of second phase particles in grain refinement induced by heavy plastic deformation. In the case of age hardenable alloys, the presence of precipitates prior to HE processing decreases the rate of grain refinement [8]. One should also note, that some second phase particles are almost always present in the majority of engineering

materials, including those which are theoretically single phased. As HE processing changes the distribution, but frequently also the size and shape of second phase particles, it is expected to impart better fracture characteristics, when controlled by relatively large particles and/or their clusters, and give enhanced corrosion resistance because of the geometry of particles in the near surface zone.

The recent development in HE processing of metals is already quite promising, nevertheless there is still much room for significant improvement. First, the final diameter-thickness of extruded products can be increased by the hydrostatic extrusion of pre-extruded-multi-wire billets [30]. Second, the heating during processing and post-processing cooling can be utilized for thermal treatment of the deformed hardenable alloys. Third, other post-processing conditions, e.g., soaking in pressurized media, can be applied to optimize the microstructure and properties of the processed elements. All these options for enhancement of the HE processing are currently being investigated in a program jointly executed by Warsaw University of Technology and the Institute for High Pressure Physics of the Polish Academy of Sciences.

**Acknowledgement** This work was supported by the Polish Ministry of Science and Higher Education (Grant No 3T08A 06430).

## References

1. Valiev RZ, Islamgaliev RK, Alexandrov IV (2000) *Prog Mater Sci* 45:103. doi:[10.1016/S0079-6425\(99\)00007-9](https://doi.org/10.1016/S0079-6425(99)00007-9)
2. Hughes DA, Hansen N (2000) *Acta Mater* 48:2985. doi:[10.1016/S1359-6454\(00\)00082-3](https://doi.org/10.1016/S1359-6454(00)00082-3)
3. Valiev RZ, Langdon TG (2006) *Prog Mater Sci* 51:881. doi:[10.1016/j.pmatsci.2006.02.003](https://doi.org/10.1016/j.pmatsci.2006.02.003)
4. Sakai G, Horita Z, Langdon TG (2005) *Mater Sci Eng A* 393:344. doi:[10.1016/j.msea.2004.11.007](https://doi.org/10.1016/j.msea.2004.11.007)
5. Richert M, Liu Q, Hansen N (1999) *Mater Sci Eng A* 260:275. doi:[10.1016/S0921-5093\(98\)00988-5](https://doi.org/10.1016/S0921-5093(98)00988-5)
6. Cherukuri B, Nedkova TS, Srinivasan R (2005) *Mater Sci Eng A* 410–411:394. doi:[10.1016/j.msea.2005.08.024](https://doi.org/10.1016/j.msea.2005.08.024)
7. Kurzydłowski KJ (2006) *Mat Sci Forum* 503–504:341
8. Lewandowska M, Pachla W, Kurzydłowski KJ (2007) *Int J Mat Res [formely Z Metallkd]* 98:172
9. Kurzydłowski KJ, Lewandowska M (2007) *Mat Sci Forum* 561–565:913
10. Lewandowska M (2006) *Solid State Phenom* 114:109
11. Lewandowska M (2006) *J Microsc* 224:34. doi:[10.1111/j.1365-2818.2006.01651.x](https://doi.org/10.1111/j.1365-2818.2006.01651.x)
12. Zdunek J, Widlicki P, Garbacz H, Mizera J, Kurzydłowski KJ (2006) *Solid State Phenom* 114:171
13. Widlicki P, Garbacz H, Lewandowska M, Pachla W, Kulczyk M, Kurzydłowski KJ (2006) *Solid State Phenom* 114:145
14. Kulczyk M, Pachla W, Świderska-Środa A, Krasilnikov N, Diduszko R, Mazur A et al (2006) *Solid State Phenom* 114:51
15. Topolski K, Garbacz H, Pachla W, Kurzydłowski KJ (2007) *Adv Mat Sci* 7:114
16. Garbacz H, Lewandowska M, Pachla W, Kurzydłowski KJ (2006) *J Microsc* 223:272. doi:[10.1111/j.1365-2818.2006.01646.x](https://doi.org/10.1111/j.1365-2818.2006.01646.x)

17. Lewandowska M, Krawczyńska A, Kurzydłowski KJ (2008) *J Nucl Mater* (accepted)
18. Kulczyk M (2007) PhD thesis, Warsaw University of Technology
19. Kulczyk M, Pachla W, Mazur A, Sus-Ryszkowska M, Krasilnikov N, Kurzydłowski KJ (2007) *Mat Sci Poland* 25:991
20. Kamikawa N, Tsuji N, Huang X, Hansen N (2006) *Acta Mater* 54:3055. doi:[10.1016/j.actamat.2006.02.046](https://doi.org/10.1016/j.actamat.2006.02.046)
21. Liu Q, Huang X, Lloyd DJ, Hansen N (2002) *Acta Mater* 50:3789. doi:[10.1016/S1359-6454\(02\)00174-X](https://doi.org/10.1016/S1359-6454(02)00174-X)
22. Kurzydłowski KJ, Ralph B (1995) Quantitative description of materials microstructure. CRC Press, Boca Raton
23. Apps PJ, Bowen JR, Prangnell PB (2003) *Acta Mater* 51:2811
24. Murayama M, Horita Z, Hono K (2001) *Acta Mater* 49:21. doi:[10.1016/S1359-6454\(00\)00308-6](https://doi.org/10.1016/S1359-6454(00)00308-6)
25. Kumar KS, Van Swygenhoven H, Suresh S (2003) *Acta Mater* 51:5743. doi:[10.1016/j.actamat.2003.08.032](https://doi.org/10.1016/j.actamat.2003.08.032)
26. Garbacz H, Grądzka-Dahlke M, Kurzydłowski KJ (2007) *Wear* 263:572. doi:[10.1016/j.wear.2006.11.047](https://doi.org/10.1016/j.wear.2006.11.047)
27. Garbacz H, Pisarek M, Kurzydłowski KJ (2007) *Biomol Eng* 24:559. doi:[10.1016/j.bioeng.2007.08.007](https://doi.org/10.1016/j.bioeng.2007.08.007)
28. Pisarek M, Kędzierzawki P, Janik-Czachor M, Kurzydłowski KJ (2007) *Electr Comm* 9:2463. doi:[10.1016/j.elecom.2007.07.028](https://doi.org/10.1016/j.elecom.2007.07.028)
29. Klassek D, Suter T, Schmutz P, Pachla W, Lewandowska M, Kurzydłowski KJ et al (2006) *Solid State Phenom* 114:189
30. Pachla W, Kulczyk M, Świderek-Środa A, Lewandowska M, Garbacz H, Mazur A et al (2006) Proc of 9th Int Conf on Mat. Forming ESAFORM-2006, Glasgow, UK, April 26–28, 2006, p 535